

Optimizing Region Selection for Weakly Supervised Object Detection

Wenhui Jiang¹, Thuyen Ngo², B.S. Manjunath², Zhicheng Zhao¹, Fei Su¹

¹ Beijing University of Posts and Telecommunications, Beijing, China

² University of California, Santa Barbara, CA, USA

Abstract

Training object detectors with only image-level annotations is very challenging because the target objects are often surrounded by a large number of background clutters. Many existing approaches tackle this problem through object proposal mining. However, the collected positive regions are either low in precision or lack of diversity, and the strategy of collecting negative regions is not carefully designed, neither. Moreover, training is often slow because region selection and object detector training are processed separately. In this context, the primary contribution of this work is to improve weakly supervised detection with an optimized region selection strategy. The proposed method collects purified positive training regions by progressively removing easy background clutters, and selects discriminative negative regions by mining class-specific hard samples. This region selection procedure is further integrated into a CNN-based weakly supervised detection (WSD) framework, and can be performed in each stochastic gradient descent mini-batch during training. Therefore, the entire model can be trained end-to-end efficiently. Extensive evaluation results on PASCAL VOC 2007, VOC 2010 and VOC 2012 datasets are presented which demonstrate that the proposed method effectively improves WSD.

1. Introduction

Object detection aims at predicting the category as well as the bounding box locations for each object instance. Recent breakthroughs in object detection [6, 12, 16, 22, 23] are driven by supervised approaches with deep convolutional neural networks (CNNs). However, strong supervision requires a large number of bounding box annotations, which are relatively hard to obtain [20, 30, 32]. In contrast, weakly-supervised detection (WSD) assumes that only image-level labels indicating the presence or absence of an object category are available for training.

Most existing methods formulate the weakly supervised detection task as a multiple instance learning (MIL) prob-

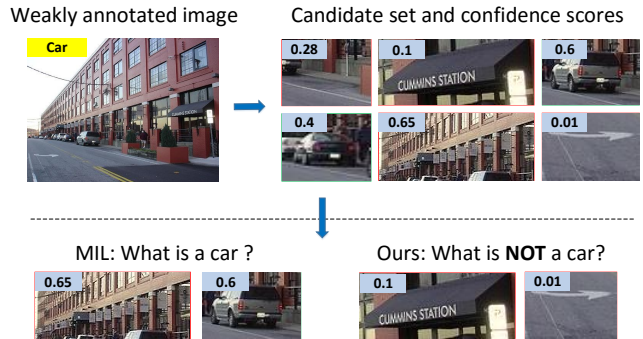


Figure 1: Comparison of our work with existing multiple instance learning (MIL) based approaches on positive region mining. Green boxes indicate true positive regions while the red ones represent backgrounds. MIL-based models select positive regions from a noisy candidate set directly, which usually results in low accuracy and diversity (bottom-left). In contrast, we progressively remove clear background regions from the candidate set (bottom-right), which reduces object-background ambiguity effectively and helps object localization easier and accurate. On VOC2007, our strategy improves the detection accuracy by 5.8% over the state-of-the-art MIL-based model [34].

lem [3, 5, 24, 28, 34]. Under MIL paradigm, learning usually alternates between two steps. (a) Estimating CNN-based object detectors based on a fixed set of training regions. (b) Updating the training set using the learned object detectors. Although existing methods have shown promising results, these methods have two major drawbacks.

1. The collected positive sets are either noisy or lack of diversity (see Figure 1 for an example). As a result, the performance of the learned object detectors is limited.
2. No model updates are made in step (b)—the CNN-based object detectors are frozen for at least one epoch for updating on the entire training set. This largely slows down the training process.

In this paper, we attempt to address two major questions.

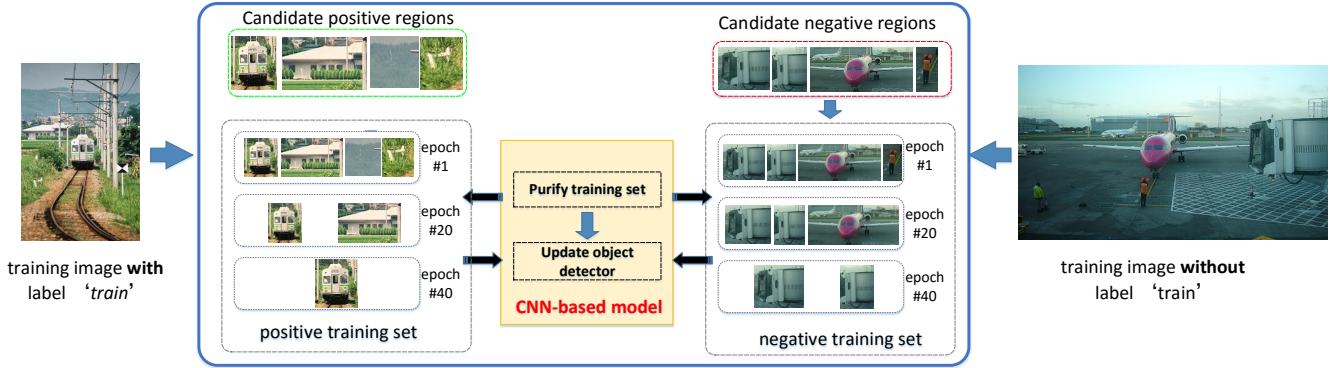


Figure 2: A brief illustration of the relevant region selection process. At the beginning, for a given object category (e.g., “train”), the positive training set starts from all the regions of the images with positive labels, and the negative training set begins with all the regions of the images with negative labels. During the training iteration, obvious negative samples inside positive set are filtered out, leading to a purified positive set. At the same time, the easy negative samples inside negative set are also removed, leading to a discriminative negative set.

First, how to select positive and negative regions for training CNN-based object detectors under weak supervision. Ideally, the selected regions should be accurate and discriminative. Second, how region selection can be combined with the learning of object detectors so that both parts can be jointly optimized during training.

Towards the first goal, we propose an optimized region selection strategy. It consists of positive and negative region selection. To select positive regions, *our key observation is that it is hard to identify all true positives directly for object detectors*. Essentially, the main difficulty arises from the large ambiguity between small target objects and large background clutters. In contrast, as shown in Figure 1, *it is relatively easy to find out most of the background regions for most models*. Hence, we progressively update the positive set by filtering out easy backgrounds while training the object detectors. As the number of background regions decreases gradually, object-background ambiguity can be reduced effectively and localizing true positive regions becomes easier. We also investigate a class-specific hard negative selection strategy to improve the discrimination of negative training set. Unlike positive labels, negative labels provide strong supervision, i.e., all of the regions are negative samples if the image-level label is negative. As has been revealed in previous studies [10, 26], the “hard” samples (which are wrongly determined by the detector) are more discriminative compared with the “easy” ones. Therefore, we select hard regions inside negatively-labeled images as negative samples. The negative samples are class-specific, hence they can carry more discriminative information. This is illustrated in Figure 2.

To address the second issue, we incorporate both region selection and object detector learning into a unified CNN framework. Specifically, in each stochastic gradient descent

(SGD) mini-batch, the region selection module samples the class-specific training regions through the forward process, then the object detectors are updated on top of them. Therefore, the proposed model can be updated as frequently as the networks without region selection [4].

Our proposed approach is simple to implement. We evaluate and compare the performance of our method on three challenging datasets, the PASCAL VOC 2007, VOC 2010 and VOC 2012 [9]. Our model achieves the detection average precision (mAP) of 37.4% on VOC 2007, which is 5.6% higher than the baseline without region selection [4], and 5.8% higher than the best MIL-based model [34]. On VOC 2010 and VOC 2012, we obtain the precision of 36.0% and 33.6%, which significantly outperform other state-of-the-art methods.

Summarizing, the main contributions of our work are:

1. We propose a progressive pruning strategy for region selection. This algorithm leads to purified positive sets and discriminative negative sets, both of which improved detection performance.
2. Our model addresses both object detector learning and region selection within a unified CNN network, which allows for end-to-end training. Although region selection has been discussed in several works [1, 24, 27] before, we apply it to build a novel CNN network for weakly supervised detection, which is, to the best of our knowledge, unique to our work.

2. Related work

2.1. Multiple Instance Learning

There have been a number of recent works addressing weakly-supervised detection (WSD) through the Multiple

Instance Learning (MIL) paradigm [1, 3, 5, 24, 29, 34]. Several methods focus on selecting precise positive regions and discriminative negative regions to improve WSD. For example, Andrews et al. [1] pick out the most confident region from each positive (or negative) image as the positive (or negative) training sample. Siva et al. [27] localize the positive regions which have maximal distances to their nearest neighbors within negative images. Ren et al. [24] propose a bag-splitting algorithm that iteratively includes hard negative regions from positively-labeled images into negative training set, and randomly selects negative samples from the set.

Our work is inspired by previous work on selecting training regions, but different in three aspects. First, our model focus on a sparse collection of positive regions, which improves the diversity of the positive training samples and avoids the impact from noisy backgrounds as well. Second, instead of selecting easiest negative region [1] or randomly [24], we collect class-specific hard samples as negative regions which carry more discriminative information. Third, different from most MIL-based methods which process region selection in an offline manner, our proposed region selection strategy can be processed in each SGD mini-batch, which makes the training efficient.

2.2. CNN for weakly supervised detection

As another line of research, Oquab et al. [18, 19], Zhou et al. [35, 36] and Bency [2] show that CNN for image classification automatically learns object activation maps, where the target objects can be coarsely localized. In these works, the activation maps can be learned end-to-end from image-level labels. However, they require a separate post-processing step to obtain the final localization.

The most similar approach to ours is the weakly supervised deep detection network (WSDDN) by Bilen et al. [4]. In [4], a two-stream CNN network is proposed—one stream for region classification and the other stream for detection. However, WSDDN has two major drawbacks. On one hand, it attempts to train object detectors from the whole noisy candidate region set. On the other hand, it tends to capture only the simplest negative samples. While our network architecture is similar to WSDDN [4], the region selection module encourages our network to focus a sparse collection of accurate positive regions and discriminative negative regions, which improves the distinction of the learned object detectors. This is explained in greater detail and verified experimentally in section 5.4. In addition, such improvement does not involve extra parameters compared with WSDDN [4].

2.3. Online batch selection

There are several methods [17, 26] that select hard training samples for training CNNs under strong supervision.

The hard samples are chosen based on losses. Our work is motivated by [17, 26]. However, under weak supervision, the relevant regions can not be simply defined based on losses, therefore it is not straightforward to adapt existing methods to WSD. Moreover, existing methods [17, 26] only select class-independent hard samples. In contrast, in our work, the selected training samples are class-specific, which carries more discriminative information.

3. WSD with region selection

In this section, we briefly describe our method for weakly supervised detection. The model is designed to automatically select relevant training regions in each SGD mini-batch, and simultaneously performs end-to-end learning of a deep object detector from the selected regions.

Given K training images $\{I^k\}_{k=1}^K$, each image I^k has a set of candidate object regions $B^k = \{b_i^k\}_{i=1}^{N^k}$. Let $\mathbf{y}^k = [y_1^k, \dots, y_C^k]$ represents its image-level label vector, where C is the total number of object categories and $y_c^k \in \{+1, 0\}$ denotes whether this image contains the c -th object category. Based on the assumption of Multiple Instance Learning, if $y_c^k = +1$, then at least one region $b_i^k \in B^k$ is a positive sample for the c -th category. Otherwise, all of the regions in B^k are negative samples.

Let $\mathbf{p}_i^k = [p_{i,1}^k, \dots, p_{i,C}^k]$ denote the estimated class probability vector for candidate object region b_i^k . Denote $\{\mathbf{v}_i^k\}_{i=1}^{N^k}$ as the weighting vectors for all regions, where $\mathbf{v}_i^k = [v_{i,1}^k, \dots, v_{i,C}^k]$ and $v_{i,c}^k \in [0, 1]$ represents the sample importance of region b_i^k for training the c -th object category. Different from \mathbf{p}_i^k which is only determined by each region b_i^k individually, \mathbf{v}_i^k determines the sample importance by comparing among all the regions inside the image I^k . The correct and discriminative regions will be selected and learned to have high values to emphasize their sample importance. The rest regions will result in $v_{i,c}^k = 0$. In this work, we model \mathbf{v}_i^k and \mathbf{p}_i^k with an importance weighting module and a object classification module, respectively. Assume \mathbf{v}_i^k and \mathbf{p}_i^k are determined by parameter vector θ . We can define a per-category per-image cross entropy loss \mathcal{L} :

$$\begin{aligned} \mathcal{L}[y_c^k, f(B^k; \theta)] = & -y_c^k \log(f(B^k; \theta)) \\ & - (1 - y_c^k) \log(1 - f(B^k; \theta)) \end{aligned} \quad (1)$$

where $f(B^k; \theta)$ is the aggregation function [8, 21] which aggregates the region-level class probabilities into image-level annotation scores:

$$\begin{aligned} f(B^k; \theta) = & \sum_{i=1}^{N^k} (v_{i,c}^k \cdot p_{i,c}^k) \\ \text{s.t. } \sum_{i=1}^{N^k} v_{i,c}^k = & 1, \quad \sum_{c=1}^C p_{i,c}^k = 1 \end{aligned} \quad (2)$$

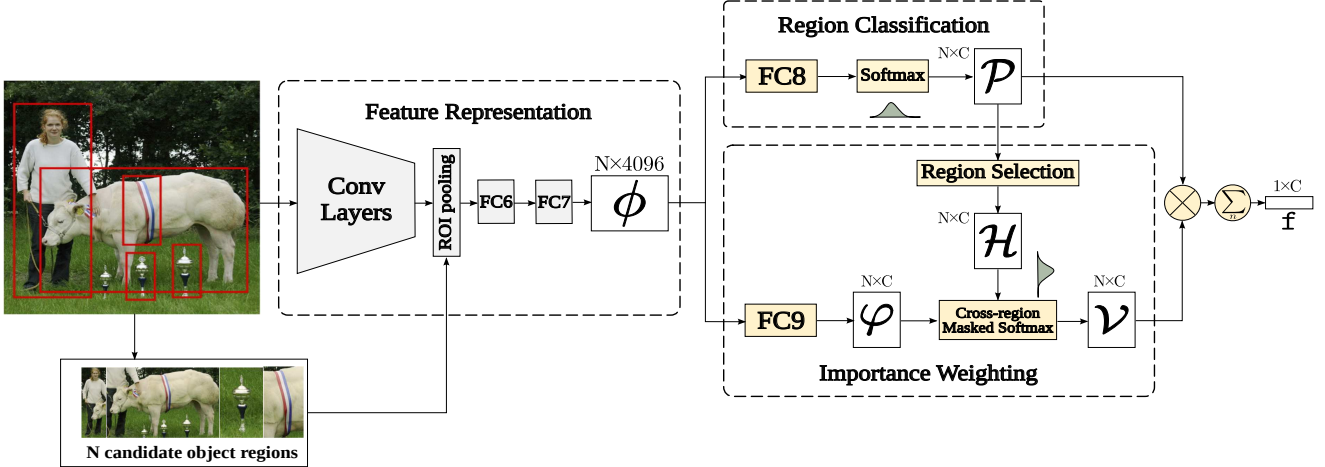


Figure 3: Overall architecture of our proposed model. It mainly consists of three modules: 1) a feature representation module which extracts a deep feature vector ϕ for each candidate object region, 2) a region classification module which estimates class probability vector \mathbf{p} for each region individually, and 3) an importance weighting module, which selects relevant training regions and estimates sample importance vector \mathbf{v} for each region. Please see Section 3 and 4 for detailed illustrations.

It is worth mentioning that the constraint on \mathbf{v}_i^k is applied across all the regions, which is different from that of \mathbf{p}_i^k . Such constraint is designed to allocate higher weights on only important regions.

In our model, the final goal is to learn the model parameter vector θ according to the summed loss:

$$\theta = \operatorname{argmin}_{\theta} \sum_{c=1}^C \sum_{k=1}^K \mathcal{L}[y_c^k, f(B^k; \theta)] \quad (3)$$

We propose a novel network to model Eqs. (1)-(3), which will be explained in detail in the following section.

4. Network architecture

4.1. Overview

Figure 3 shows the architecture of the proposed model. Our model is built based on weakly supervised deep detection network (WSDDN) architecture [4]. It takes an image I^k and a set of candidate regions $B^k = \{b_i^k\}_{i=1}^{N^k}$ as inputs (for simplicity, we drop the superscript k in the rest of the paper). It mainly consists of three modules: 1) a feature representation module, 2) a region classification module, 3) an importance weighting module. The feature representation module extracts fixed-size deep descriptor ϕ_i for each candidate region b_i . The region classification module maps ϕ_i to a class probability vector \mathbf{p}_i for each region individually. The importance weighting module selects relevant positive and negative regions among all the regions, and outputs a weighting vector \mathbf{v}_i which reflects relative importance of regions for training the entire network. The learning of

the three modules is supervised by image-level annotation \mathbf{y} only. In the following subsections, we will explain these three modules in more details.

4.2. Feature representation

This module is built based on Fast RCNN architecture [12]. It first takes an image I of arbitrary size as input, extracting image feature maps \mathbf{G} using a stack of convolutional layers (e.g., five convolutional layers as in AlexNet [15]). Then, given each candidate region b_i , a fixed-size region-level feature map is extracted through ROI Pooling layer [12] on \mathbf{G} . Two fully connected layers (FC6 and FC7) are followed to output a fixed-length feature vector ϕ_i .

4.3. Region classification

This module is designed to classify b_i into object categories. Towards this goal, we apply an additional fully connected layer (FC8) that maps ϕ_i to a C dimensional output ϕ_{8i} . As each region could represent at most one object, we apply conventional softmax operator to normalize ϕ_{8i} to a class probability vector \mathbf{p}_i .

4.4. Importance weighting

This is the most important part of our model. It mainly contains two components, one is to select class-specific training regions, the other one is to impose soft sample importance on the selected regions. The module outputs weighting vectors $\{\mathbf{v}_i\}_{i=1}^N$, which reflect the relative sample importance of each region in image I .

Region selection: For each object category c , we choose positive regions from images with positive label, and negative regions from images with negative labels. We consider the following circumstances:

1. When $y_c = +1$, if the estimated score $p_{i,c}$ is low, then it is very likely that b_i comes from the background, and therefore should be removed from the positive training set ($v_{i,c} = 0$). The rest regions are candidate true positives and are taken as positive training set ($v_{i,c} > 0$).
2. When $y_c = 0$, if the estimated score $p_{i,c}$ is high, then b_i is wrongly classified, and is therefore selected as a negative region ($v_{i,c} > 0$). This coincides with the idea for hard negative mining [10], which indicates that "hard samples" are more discriminative under strong supervision.

In summary, only the regions with high probability scores $p_{i,c}$ are selected as training samples. Therefore, for each object category, we rank the regions based on probability scores $p_{i,c}$, and pick up the top M_{pc} or M_{nc} highest scoring regions as positive or negative regions according to the image-level labels. For simplicity, we assume the value of M_{pc} and M_{nc} are independent of object categories. Therefore, we denote M_{pc} and M_{nc} as M_p and M_n , respectively. Formally, region selection can be processed according to:

$$\begin{aligned} \{h_{i,c}\}_{i=1}^N &= \underset{\mathbf{h}}{\operatorname{argmax}} \sum_{i=1}^N (h_{i,c} \cdot p_{i,c}) \\ \text{s.t. } \sum_{i=1}^N h_{i,c} &= y_c M_p + (1 - y_c) M_n \end{aligned} \quad (4)$$

where $\mathbf{h}_i = [h_{i,1}, \dots, h_{i,C}]$ represents the selection indicator vector for region b_i , $h_{i,c} \in \{1, 0\}$ indicates the selection of b_i for training the c -th object category or not.

For different object categories, the training samples might be different. Such class-specific region selection strategy carries more discriminative information, because each class can select the most relevant regions against the other classes.

Soft importance weighting: We apply a cross-region soft weighting strategy to impose different sample importance on the selected regions. Specifically, we append another fully connected layer (FC9) which maps ϕ_i to a C dimensional output φ_i . Then, φ_i is connected to a cross-region masked softmax layer with \mathbf{h}_i , which is defined as:

$$v_{i,c} = \frac{h_{i,c} \exp(\varphi_{i,c})}{\sum_{j=1}^N h_{j,c} \exp(\varphi_{j,c})} \quad (5)$$

As we can see, $v_{i,c}$ compares the relative sample importance of each region for training the c -th object category.

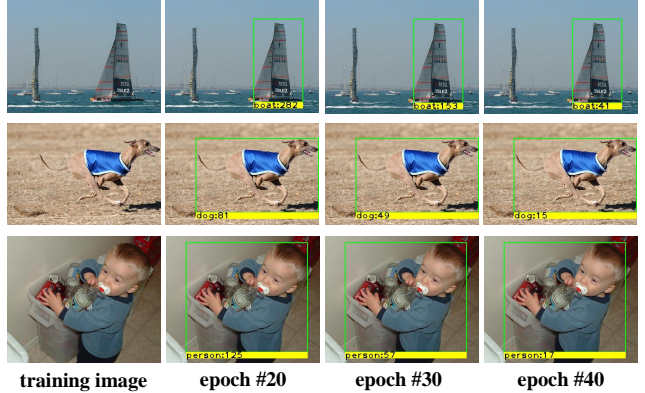


Figure 4: Update of the rankings of sampled positive regions during training. In each yellow rectangle, we list the ranking of the labelled region among all proposals inside the given image based on the class probability score.

If a certain region is masked by $h_{i,c}$, $v_{i,c}$ outputs 0. This region selection strategy proceeds within a single CNN forward operation. During backward operation, only the selected regions contribute to gradient propagation. Therefore, the whole model can be updated as frequently as the same network without region selection.

4.5. Progressive pruning

The parameter M_p controls the pace at which the model learns from positive samples. In this paper, we propose to adjust M_p dynamically as the training processes. Intuitively, when the learned detectors are weak, we set M_p to a large number so that high recall rates are retained. As the detectors grow mature, more positive regions are ranked in the top (see Figure 4 for visual examples), we gradually decrease M_p to improve the precision of the positive set. Specifically, M_p is set to N (the total number of candidate regions inside the image) when the training begins. After 20 epoches, we set M_p to 1024, and progressively reduce M_p by half every N_e epoches until M_p reaches a pre-defined threshold M_{pt} . N_e is obtained according to:

$$N_e = \frac{20}{\log_2(1024/M_{pt}) + 1} \quad (6)$$

Since negative image labels provide strong supervision, we keep M_n fixed during the training process. In practice, we set both M_{pt} and M_n to 128, which is a typical setting for mini-batch selection.

5. Experiments

5.1. Datasets

We evaluate our model on three large image datasets, the PASCAL VOC 2007, VOC 2010 and VOC 2012. The VOC

VOC 2007 dataset has labels for 20 object categories and contains 2501 images for training, 2510 images for validation and 4952 images for testing. VOC 2010 and VOC 2012 share the same class labels. VOC 2010 includes 4998 images for training, 5105 images for validation and 9637 images for testing. VOC 2012 contains 5717 training images, 5823 validation images and 10991 test images. These datasets contain both image-level labels and object location annotations. For weak supervision, we only utilize the image-level labels for training. Following [2, 4, 5, 34], we use both train and val splits as the training set and test split as our test set for VOC 2007 and VOC 2010. For VOC 2012, we use train split as the training set and val split as the test set.

5.2. Evaluation metrics

We use two metrics to evaluate localization performance. First, we quantify localization performance in the training set with the Correct Localization (CorLoc) measure [7]. CorLoc is the percentage of images in which the bounding-box returned by the algorithm correctly localizes an object of the target class. It reflects the top-1 accuracy of positive region selection strategy. Second, we measure the performance of object detectors using mean average precision (mAP) in the test set, as standard in PASCAL VOC. For both metrics, we consider that a bounding box is correct if it has an intersection-over-union (IoU) ratio of at least 0.5 with a ground-truth object instance annotation.

5.3. Implementation details

Our network is built with caffe [13]. We adopt AlexNet [15] as the backbone architecture. It is pre-trained on ImageNet [25] to initialize the convolutional layers and the two fully connected layers (FC6 and FC7). Rest of the layers are initialized randomly as in [12].

We extract candidate object regions with EdgeBoxes (EB) [37] for each image. We fine-tune the network on the target datasets. Each mini-batch contains all the ROIs from one image. We adopt multi-scale training. Specifically, the longer side of images is resized to a random scale s ($s \in \{480, 576, 688, 864, 1200\}$) while the aspect ratio is kept unchanged. We also apply random horizontal flips to the images for data augmentation. The experiments are run for 40 epochs.

At test time we take $v_{i,c} \cdot p_{i,c}$ as the final class confidence score for region b_i . As with [4], we average the outputs of 10 images (i.e., the 5 scales as in training and their flips). The results are post-processed by bounding box voting [11] and non-maximum suppression (NMS) using a threshold of 0.6 IoU.

5.4. The impact of region selection

Settings: To analyze the effects of region selection, we train the system with different values of M_p and M_n using VOC

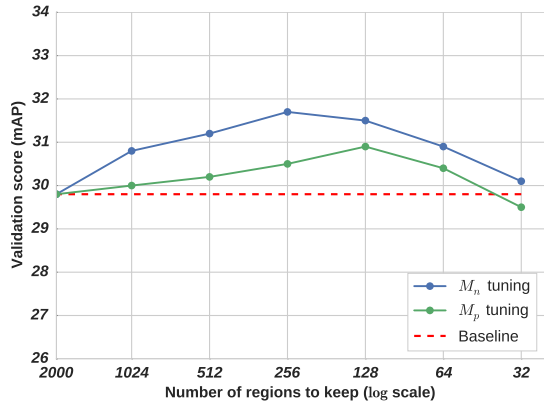


Figure 5: Detection performance on VOC 2007 holdout images with different values of M_p (number of selected positive regions) and M_n (number of selected negative regions). Green curve: varying M_p while fixing M_n . Blue curve: varying M_n while fixing M_p . Red dash line: baseline (without region selection). See section 5.4 for more details.

2007 training set and measure the performance on 500 hold-out images randomly selected from the validation set.

Baseline: We remove the region selection module as the baseline. This is equivalent to setting M_p and M_n to N for the entire training process. The baseline model achieves a mAP of 29.8% on the holdout validation set.

Observation: First of all, we demonstrate the importance of positive region selection. Toward this goal, we fix $M_n = N$ (which disable negative region selection), and gradually reduce M_p from N to 32 to see how positive region selection impacts WSD. As is shown in Figure 5 (in green curve), when M_p varies from N to 32, the performance first monotonically increases, which demonstrates positive region selection helps improve object detection performance. When $M_p = 128$, the mAP reaches the peak 30.9%. Then the performance drops to 29.5%. Second, we show the efficacy of negative region selection. In this experiment, we fix $M_p = N$ and decrease M_n from N to 32. As is shown in Figure 5 (in blue curve), the mAP monotonically increases until it reaches the peak, then the performance drops again when M_n continues decreasing. Setting M_n to 256 leads to close-to-optimal result.

Analysis: It is important to discuss why relevant region selection helps improve the performance of object detection. We first look into the baseline model. As we can see from Eqs. (1) - (2), when $y_c = 1$, regions with high classification score $p_{i,c}$ naturally encourage $v_{i,c}$ to be high as well, while regions with low $p_{i,c}$ will result in low $v_{i,c}$. With VOC 2007 train set, when the candidate regions are sorted by $p_{i,c}$, we observe the long-tail phenomenon — 84.17% of the impor-

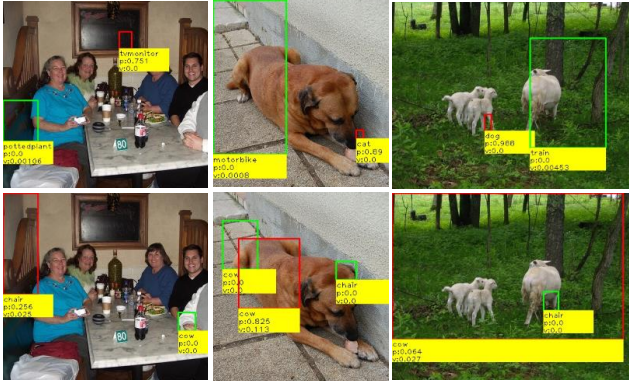


Figure 6: Visualization of the negative regions. The green bounding boxes represent true negatives while the red boxes depict false negatives. p represents the classification score and v represents the weighting score. Top row shows the results from the baseline (without negative region selection), and the bottom row shows the results from our proposed model (with negative region selection).

tance weights are from the top-128 regions. We believe that suppressing the weights from regions ranking 128 and beyond can benefit WSD in two aspects: 1) more supervision flows towards true positive regions (most of them rank top-128), 2) less supervision mis-flows towards false negative regions (ranking 128 and beyond). As the weights occupied from 512 and beyond are ignorable, when M_p drops from N to 512, the performance boost is very limited. When we further reduce M_p to 128, the mAP improves significantly. When M_p comes to 32, as more true positive regions are filtered out (which leads to average recall rates decrease), the performance drops drastically.

We also investigate the weight distribution when $y_c = 0$. We observe that only 10.08% weights come from the top-128 ranked regions. This is not surprising since the baseline model treats the supervision from both positive label and negative label equally, therefore it puts more weights on easy negative regions instead of hard ones. The negative region selection benefits WSD by re-assigning more weights on hard regions, and suppressing the weights on those correctly identified negative regions at the same time. For a better illustration, we visualize the “hardest negative regions” identified by our model (with negative region selection) and the baseline (without negative region selection) in Figure 6. In the examples, all the red boxes are false negatives with high probability scores, and green boxes are true negatives. However, for the baseline method (top row), the false negatives are assigned close-to-zero weights, indicating they are not important as negative regions for training object detectors. On the contrary, the true negatives are assigned high weights. In comparison, with negative region selection (bottom row), the hard negative regions are assigned higher

Table 1: Quantitative comparison between our model and other WSDN variants on the PASCAL VOC 2007 test set.

	Method	mAP
(a)	WSDN [4]	31.5
(b)	WSDN + Sc [4]	33.4
(c)	WSDN + Sc + Reg [4]	34.5
(d)	AttentionNet [31]	34.5
(e)	ContextLocNet [14]	36.3
(f)	Ours	37.4

weights. As a result, when we reduce M_n from N to 256, the performance improves consistently. When we further decrease M_n to 32, the detection performance drops. This is probably due to the decrease in the diversity of negative regions within a mini-batch.

5.5. Compare with other WSDN variants

Our network is similar to the weakly supervised deep detection network (WSDN) by Bilen et al. [4] in network architecture. The major difference is that we replace the detection branch in WSDN [4] with a elaborately designed region selection module. Concurrent with our work, there are also a series of variants of WSDN [14, 31]. We compare these approaches in Table 1.

As presented in Table 1, our model improves significantly (+5.9%) over the WSDN baseline [4] (row (a)), and also outperforms other WSDN variants. In [4] Bilen et al. extend WSDN with objectness scaling (row (b)) and a new regularization term (row (c)), boosting their result to 34.5% in mAP (without model ensemble). Our method still outperforms such variants. In addition, objectness scaling (Sc) cannot be applied to proposal methods which provide no objectness scores for each region (e.g., Selective Search [33]). In contrast, our proposed region selection module does not require extra objectness scores. Our model also outperforms recent variants AttentionNet [31] (row (d)) and ContextlocNet [14] (row (e)) for object localization under weak supervision.

5.6. Compare with state-of-the-art

We also compare the detection results of our method with recent state-of-the-art WSD methods, including MIL-based methods and other CNN-based models. For a fair comparison, we also re-implement WSDN [4] as the baseline by removing the region selection module.

Table 2 shows performance comparison in terms of CorLoc [7] on the PASCAL VOC 2007 trainval set. Our method achieves 57.3% of average CorLoc for all the 20 categories, outperforming all the alternatives. It indicates that our model achieves the best performance of localizing true positive regions in the training set, which in another way verifies the effectiveness of the proposed region selection module.

Table 2: Quantitative comparison in terms of correct localization (CorLoc) on the PASCAL VOC 2007 trainval set.

Method	aero	bike	bird	boat	bottle	bus	car	cat	chair	cow	table	dog	horse	mbike	pers	plant	sheep	sofa	train	tv	mean
Bilen [3]	66.4	59.3	42.7	20.4	21.3	63.4	74.3	59.6	21.1	58.2	14.0	38.5	49.5	60.0	19.8	39.2	41.7	30.1	50.2	44.1	43.7
Cinbis [5]	65.3	55.0	52.4	48.3	18.2	66.4	77.8	35.6	26.5	67.0	46.9	48.4	70.5	69.1	35.2	35.2	69.6	43.4	64.6	43.7	52.0
Wang [34]	80.1	63.9	51.5	14.9	21.0	55.7	74.2	43.5	26.2	53.4	16.3	56.7	58.3	69.5	14.1	38.3	58.8	47.2	49.1	60.9	48.5
Ren [24]	79.2	56.9	46.0	12.2	15.7	58.4	71.4	48.6	7.2	69.9	16.7	47.4	44.2	75.5	41.2	39.6	47.4	32.3	49.8	18.6	43.9
Bilen [4]	68.5	67.5	56.7	34.3	32.8	69.9	75.0	45.7	17.1	68.1	30.5	40.6	67.2	82.9	28.8	43.7	71.9	62.0	62.8	58.2	54.2
Kantorov [14]	83.3	68.6	54.7	23.4	18.3	73.6	74.1	54.1	8.6	65.1	47.1	59.5	67.0	83.5	35.3	39.9	67.0	49.7	63.5	65.2	55.1
Bency [2]	-	-	-	-	-	-	-	-	-	-	-	-	-	-	-	-	-	-	-	-	46.8
Baseline	69.6	68.6	58.9	26.1	40.8	68.5	70.2	36.0	11.8	58.8	36.5	41.6	66.0	82.3	17.0	46.1	56.0	39.2	70.0	67.7	51.6
Ours	76.3	72.2	61.3	44.1	41.2	70.6	78.1	53.8	12.4	60.3	55.5	51.4	70.1	86.7	25.7	46.2	59.8	40.3	70.7	68.8	57.3

Table 3: Quantitative comparison in terms of detection average precision (AP) on the PASCAL VOC 2007 test set.

Method	aero	bike	bird	boat	bottle	bus	car	cat	chair	cow	table	dog	horse	mbike	pers	plant	sheep	sofa	train	tv	mean
Bilen [3]	46.2	46.9	24.1	16.4	12.2	42.2	47.1	35.2	7.8	28.3	12.7	21.5	30.1	42.4	7.8	20.0	26.8	20.8	35.8	29.6	27.7
Cinbis [5]	39.3	43.0	28.8	20.4	8.0	45.5	47.9	22.1	8.4	33.5	23.6	29.2	38.5	47.9	20.3	20.0	35.8	30.8	41.0	20.1	30.2
Wang [34]	48.9	42.3	26.1	11.3	11.9	41.3	40.9	34.7	10.8	34.7	18.8	34.4	35.4	52.7	19.1	17.4	35.9	33.3	34.8	46.5	31.6
Ren [24]	41.3	39.7	22.1	9.5	3.9	41.0	45.0	19.1	1.0	34.0	16.0	21.3	32.5	43.4	21.9	19.7	21.5	22.3	36.0	18.0	25.4
Bilen [4]	42.9	56.0	32.0	17.6	10.2	61.8	50.2	29.0	3.8	36.2	18.5	31.1	45.8	54.5	10.2	15.4	36.3	45.2	50.1	43.8	34.5
Kantorov [14]	57.1	52.0	31.5	7.6	11.5	55.0	53.1	34.1	1.7	33.1	49.2	42.0	47.3	56.6	15.3	12.8	24.8	48.9	44.4	47.8	36.3
Bency [2]	-	-	-	-	-	-	-	-	-	-	-	-	-	-	-	-	-	-	-	-	25.7
Baseline	42.1	50.8	29.7	18.5	14.7	56.8	48.3	14.2	3.1	32.3	24.2	24.7	48.9	53.8	6.6	19.9	24.8	24.2	54.5	44.5	31.8
Ours	50.1	56.1	33.4	21.1	17.8	62.0	54.2	34.2	3.1	37.1	38.5	32.5	52.9	57.0	5.3	21.4	30.0	31.6	57.4	50.2	37.4

We also present the average precision (AP) on the PASCAL VOC 2007 test set in Table 3. Our model achieves 37.4% on mAP, which outperforms all the competitors.

With optimized region selection module, the learned object detectors outperform the baseline on 19 out of 20 categories in terms of both localization and detection. Compared to the best MIL-based approaches [5, 34], we achieve significant improvements by 5.3% in Corloc, and 5.8% in mAP. For most MIL-based methods, positive training regions are selected from a noisy candidate set. We believe the large amount of background clutters within the candidate set hurt the precision of the positive training set, which leads to large object-background ambiguity. In contrast, our model progressively remove the noisy backgrounds from the positive set. As a result, the precision of the collected positive set improves and high recall rate is also retained, which makes the learned object detectors discriminative. The class-specific negative set also contributes to the performance boost. Compared with CNN-based models, our model outperforms [2] by 10.5% in CorLoc and 11.7% in mAP. We notice that in [2], class activation maps are learned from the entire image. The noisy background regions inevitably affect the accuracy of the learned activation maps, and therefore may hurt detection performance. In comparison, our proposed region selection module effectively alleviates the impact from background clutters, and therefore achieves better detection performance. Visual detection results on the PASCAL VOC 2007 test set are shown in the Appendix.

We further perform experiments on the PASCAL VOC

Table 4: Quantitative comparison in terms of detection average precision (AP) on the PASCAL VOC 2010 and VOC 2012.

Method	VOC 2010	VOC 2012
Oquab [19]	-	11.7
Cinbis [5]	27.4	-
Ren [24]	-	23.8
Bency [2]	-	26.5
Baseline	29.8	29.6
Ours	36.0	33.6

2010 and VOC 2012 dataset. As presented in Table 4, our method achieves mAP of 36.0% on VOC 2010 and 33.6% on VOC 2012, significantly outperforms the state-of-the-art methods.

5.7. Visualization analysis

Visual detection results on the PASCAL VOC 2007 test set are shown in Figure 7. For each category, the box with the highest prediction score is drawn. From these examples, it can be seen that our proposed method is able to localize objects subject to great variability in scale and appearance, and even some of the small target objects are accurately discovered. Many heavily occluded objects are also successfully localized. However, several bad cases still exist. One problem is inaccurate box prediction, where only part of the true object is captured or too much background is covered. For example, when detecting a person, the bounding box is

sometimes drawn on person’s upper body. Hence, the actual performance for person detection is not desirable. Another common problem is the confusion of several visual similar classes. We believe that improving the quality of positive mining by considering both inter-class and intra-class metrics in our formulation is one way to handle these problems.

6. Acknowledgment

This work is supported by Chinese National Natural Science Foundation (61471049, 61372169, 61532018) and China Scholarship Council.

7. Conclusion

We propose an optimized region selection strategy for weakly supervised detection. This method collects purified positive training regions by progressively removing easy background clutters, which improves the precision of the positive set and retains high diversity of the training samples as well. This approach also selects discriminative negative samples by mining class-specific hard negatives. The region selection module is combined with the learning of object detectors so that both parts can be jointly optimized during training. We extensively evaluate the detection performance on the PASCAL VOC 2007, VOC 2010 and 2012 datasets. Experimental results demonstrate the region selection strategy effectively improves weakly supervised visual learning, and could become common practice for weakly supervised detection.

References

- [1] S. Andrews, I. Tsochantaridis, and T. Hofmann. Support Vector Machines for Multiple-Instance Learning. In *NIPS*, 2002. 2, 3
- [2] A. J. Bency, H. Kwon, H. Lee, S. Karthikeyan, and B. S. Manjunath. Weakly Supervised Localization using Deep Feature Maps. In *ECCV*, 2016. 3, 6, 8
- [3] H. Bilen. Weakly Supervised Object Detection with Convex Clustering. In *CVPR*, 2015. 1, 3, 8
- [4] H. Bilen and A. Vedaldi. Weakly Supervised Deep Detection Networks. In *CVPR*, 2016. 2, 3, 4, 6, 7, 8
- [5] R. G. Cinbis, J. Verbeek, and C. Schmid. Weakly Supervised Object Localization with Multi-fold Multiple Instance Learning. *TPAMI*, PP(99):1–15, 2016. 1, 3, 6, 8
- [6] J. Dai, Y. Li, K. He, and J. Sun. R-FCN : Object Detection via Region-based Fully Convolutional Networks. In *NIPS*, 2016. 1
- [7] T. Deselaers, B. Alexe, and V. Ferrari. Weakly supervised localization and learning with generic knowledge. *IJCV*, 100(3):275–293, 2012. 6, 7
- [8] T. Durand, N. Thome, and M. Cord. WELDON : Weakly Supervised Learning of Deep Convolutional Neural Networks. In *CVPR*, 2016. 3
- [9] M. Everingham, S. M. A. Eslami, L. Van Gool, C. K. I. Williams, J. Winn, and A. Zisserman. The Pascal Visual Object Classes Challenge: A Retrospective. *IJCV*, 111(1):98–136, 2014. 2
- [10] P. F. Felzenszwalb, R. B. Girshick, D. McAllester, and D. Ramanan. Object Detection with Discriminative Trained Part Based Models. *TPAMI*, 32(9):1627–1645, 2010. 2, 5
- [11] S. Gidaris and N. Komodakis. Object detection via a multi-region and semantic segmentation-aware cnn model. In *ICCV*, 2015. 6
- [12] R. Girshick. Fast R-CNN. In *ICCV*, 2015. 1, 4, 6
- [13] Y. Jia, E. Shelhamer, J. Donahue, S. Karayev, J. Long, R. Girshick, S. Guadarrama, and T. Darrell. Caffe: Convolutional architecture for fast feature embedding. *arXiv preprint arXiv:1408.5093*, 2014. 6
- [14] V. Kantorov, M. Oquab, M. Cho, and I. Laptev. Contextlocnet: Context-aware deep network models for weakly supervised localization. In *ECCV*, 2016. 7, 8
- [15] A. Krizhevsky and G. E. Hinton. ImageNet Classification with Deep Convolutional Neural Networks. In *NIPS*, pages 1–9, 2012. 4, 6
- [16] W. Liu, D. Anguelov, D. Erhan, C. Szegedy, S. Reed, C.-Y. Fu, and A. C. Berg. SSD: Single shot multibox detector. In *ECCV*, 2016. 1
- [17] I. Loshchilov and F. Hutter. Online Batch Selection For Faster Training Of Neural Networks. In *ICLR*, 2016. 3
- [18] M. Oquab, L. Bottou, I. Laptev, and J. Sivic. Learning and transferring mid-level image representations using convolutional neural networks. In *CVPR*, 2014. 3
- [19] M. Oquab, L. Bottou, I. Laptev, and J. Sivic. Is object localization for free? - Weakly-supervised learning with convolutional neural networks. In *CVPR*, 2015. 3, 8
- [20] D. P. Papadopoulos, A. D. F. Clarke, F. Keller, and V. Ferrari. Training object class detectors from eye tracking data. In *ECCV*, 2014. 1
- [21] P. O. Pinheiro and R. Collobert. From image-level to pixel-level labeling with Convolutional Networks. In *CVPR*, 2015. 3
- [22] J. Redmon, S. Divvala, R. Girshick, and A. Farhadi. You only look once: Unified, real-time object detection. In *CVPR*, 2016. 1
- [23] S. Ren, K. He, R. Girshick, and J. Sun. Faster R-CNN: Towards Real-Time Object Detection with Region Proposal Networks. In *NIPS*, 2015. 1
- [24] W. Ren, S. Member, K. Huang, and S. Member. Weakly Supervised Large Scale Object Localization with Multiple Instance Learning and Bag Splitting. *TPAMI*, 38(2):405–416, 2016. 1, 2, 3, 8
- [25] O. Russakovsky, J. Deng, H. Su, J. Krause, S. Satheesh, S. Ma, Z. Huang, A. Karpathy, A. Khosla, M. Bernstein, A. C. Berg, and L. Fei-Fei. ImageNet Large Scale Visual Recognition Challenge. *IJCV*, 115(3):211–252, 2015. 6
- [26] A. Shrivastava, A. Gupta, and R. Girshick. Training Region-based Object Detectors with Online Hard Example Mining. In *CVPR*, 2016. 2, 3
- [27] P. Siva, C. Russell, and T. Xiang. In defence of negative mining for annotating weakly labelled data. In *ECCV*, 2012. 2, 3

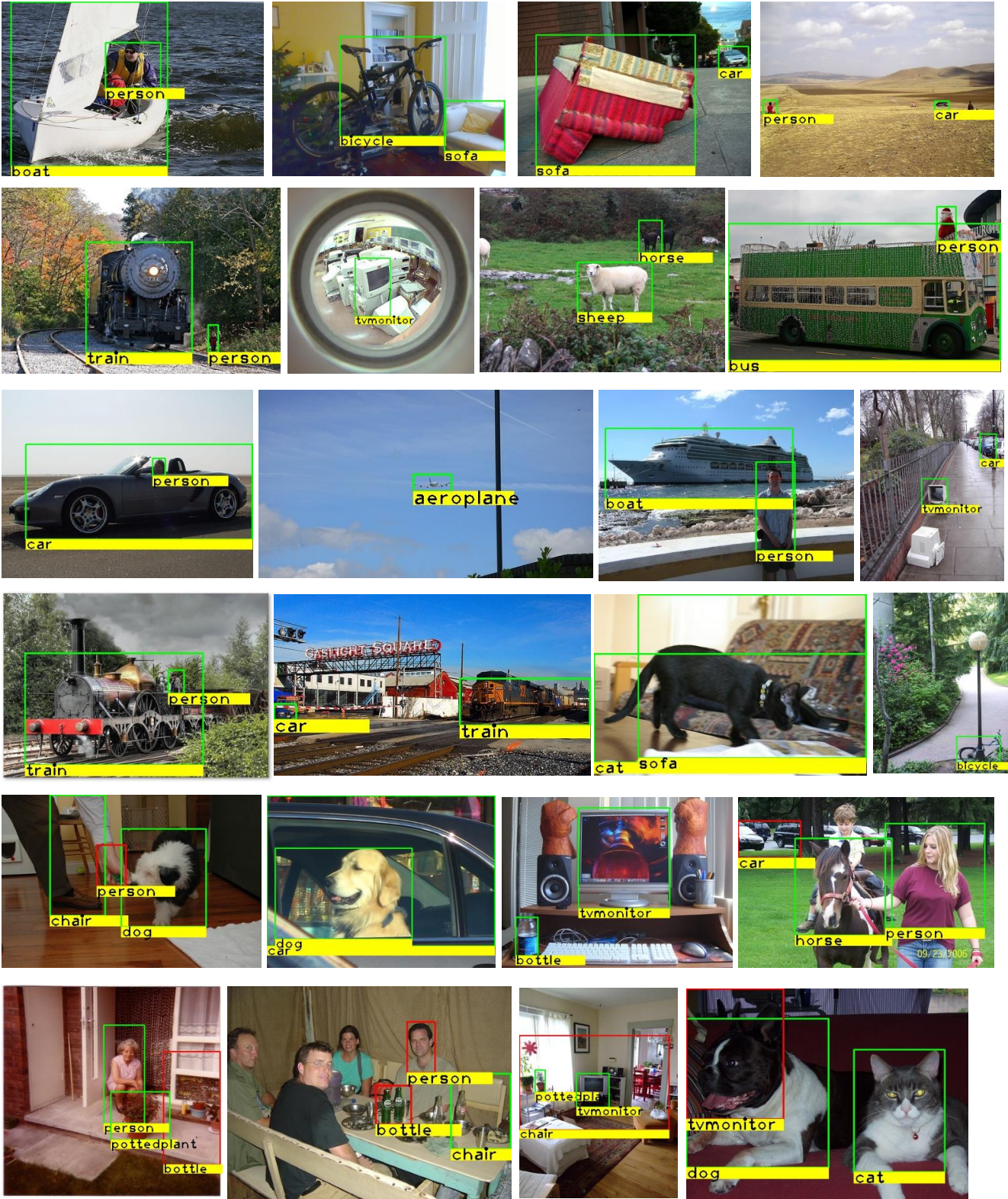


Figure 7: Sample detection results. For all the examples, we only show the top one detected region for each category. Green boxes indicate correct detections, red boxes indicate false detections.

- [28] H. O. Song, R. Girshick, S. Jegelka, J. Mairal, Z. Harchaoui, and T. Darrell. On learning to localize objects with minimal supervision. In *ICML*, 2014. [1](#)
- [29] H. O. Song, Y. J. Lee, S. Jegelka, and T. Darrell. Weakly-supervised Discovery of Visual Pattern Configurations. *NIPS*, 2014. [3](#)
- [30] H. Su, J. Deng, and L. Fei-fei. Crowdsourcing Annotations for Visual Object Detection. In *AAAI*, 2012. [1](#)
- [31] E. W. Teh and Y. Wang. Attention Networks for Weakly Supervised Object Localization. In *BMVC*, 2016. [7](#)
- [32] J. R. R. Uijlings, F. Keller, and V. Ferrari. We don't need no bounding-boxes: Training object class detectors using only human verification. In *CVPR*, 2016. [1](#)
- [33] J. R. R. Uijlings, K. E. a. Sande, T. Gevers, and a. W. M. Smeulders. Selective Search for Object Recognition. *IJCV*, 104(2):154–171, apr 2013. [7](#)
- [34] C. Wang, K. Huang, W. Ren, J. Zhang, and S. Maybank. Large-Scale Weakly Supervised Object Localization via Latent Category Learning. *TIP*, 24(4):1371–1385, 2015. [1](#), [2](#), [3](#), [6](#), [8](#)
- [35] B. Zhou, A. Khosla, A. Lapedriza, A. Oliva, and A. Torralba. Object Detectors Emerge in Deep Scene CNNs. In *ICLR*, page 12, 2015. [3](#)
- [36] B. Zhou, A. Khosla, A. Lapedriza, A. Oliva, and A. Torralba. Learning Deep Features for Discriminative Localization. In *CVPR*, 2016. [3](#)
- [37] C. L. Zitnick and P. Dollár. Edge boxes: Locating object proposals from edges. In *ECCV*, 2014. [6](#)